微生物学报
Acta Microbiologica Sinica
2024, 64(9): 3453–3473
http://journals.im.ac.cn/actamicrocn
DOI: 10.13343/j.cnki.wsxb.20240153

Research Article 研究报告

基于转录组分析的腾冲嗜热厌氧杆菌 *thiD* 的热适应机制研究

刘亚娟[1]，郑航辉[1]，刘原子[1]，陈宜军[2]，万学瑞[1]，赵春林[3]，王川[1*]，杨宇泽[2*]

1 甘肃农业大学 动物医学院，甘肃 兰州 730070
2 北京市畜牧总站，北京 100101
3 天水师范学院，甘肃 天水 741000

刘亚娟, 郑航辉, 刘原子, 陈宜军, 万学瑞, 赵春林, 王川, 杨宇泽. 基于转录组分析的腾冲嗜热厌氧杆菌 *thiD* 的热适应机制研究[J]. 微生物学报, 2024, 64(9): 3453-3473.

LIU Yajuan, ZHENG Hanghui, LIU Yuanzi, CHEN Yijun, WAN Xuerui, ZHAO Chunlin, WANG Chuan, YANG Yuze. RNA-seq reveals the role of *thiD* in the thermal adaptation of *Thermoanaerobacter tengcongensis*[J]. Acta Microbiologica Sinica, 2024, 64(9): 3453-3473.

摘　要：ThiD 在腾冲嗜热厌氧杆菌中由 *thiD* 编码，是硫铵素合成途径的关键酶。*thiD* 的结构和功能已在真菌、酵母菌和植物中得到阐明。然而，*thiD* 在嗜热生物中的功能仍不清楚。【目的】探讨腾冲嗜热厌氧杆菌的嗜热机制并揭示 *thiD* 在不同温度下的功能及在热适应调控中的作用。【方法】利用同源重组技术构建腾冲嗜热厌氧杆菌的 Δ*thiD* 株，观察并比较野生株和 Δ*thiD* 株在 50、60、75 和 80 ℃下的生长趋势。通过转录组测序分析 Δ*thiD* 株与野生株在 75 ℃的差异表达基因。通过实时荧光定量 PCR 分析比较野生株和 Δ*thiD* 株中 13 个基因和 3 个 sRNAs 在 50、60、75、80 ℃下的转录水平。【结果】成功构建了 Δ*thiD* 株，生长曲线结果显示其在 50 ℃时，Δ*thiD* 株生长速率与野生株无显著差异。然而，在 60 ℃和 75 ℃时，Δ*thiD* 株生长速度明显慢于野生株。另外，Δ*thiD* 株在 80 ℃时几乎不生长。转录组结果显示，与野生株相比，Δ*thiD* 株有 503 个差异表达基因，其中包括 278 个上调差异表达基因和 213 个下调差异表达基因。KEGG 分析表明，以下途径与热适应有关，包括硫胺素代谢、嘧啶代谢和嘌呤代谢、肽聚糖生物合成、脂肪酸代谢途径、氨基酸代谢途径、双组分系统、DNA 复制、同源重组、错配修复、磷酸转移酶系统。通过实时荧光定量 PCR 分析发现，在野生株和 Δ*thiD* 株中与嗜热机制相关的 13 个基因和 3 个 sRNAs 在特定温度下的转录

资助项目：甘肃农业大学科技创新基金(青年导师扶持基金) (GAU-QDFC-2023-04)；国家自然科学基金(31500067)
This work was supported by the Science and Technology Innovation Fund of Gansu Agricultural University (Young Mentor Support Fund) (GAU-QDFC-2023-04) and the National Natural Science Foundation of China (31500067).
*Corresponding authors. E-mail: WANG Chuan, wangchuan@gsau.edu.cn; YANG Yuze, yyz84929056@126.com
Received: 2024-03-10; Accepted: 2024-05-28; Published online: 2024-05-30

水平发生了变化。【结论】*thiD* 在腾冲嗜热厌氧杆菌热适应过程中发挥重要作用。本研究为揭示 *thiD* 在不同温度下的功能和在热适应过程中的调控机制提供实验数据和理论依据。

关键词：腾冲嗜热厌氧杆菌；*thiD*；转录组；差异表达基因；热适应

RNA-seq reveals the role of *thiD* in the thermal adaptation of *Thermoanaerobacter tengcongensis*

LIU Yajuan[1], ZHENG Hanghui[1], LIU Yuanzi[1], CHEN Yijun[2], WAN Xuerui[1], ZHAO Chunlin[3], WANG Chuan[1*], YANG Yuze[2*]

1 College of Veterinary Medicine, Gansu Agricultural University, Lanzhou 730070, Gansu, China
2 Beijing Municipal Animal Husbandry Station, Beijing 100101, China
3 Tianshui Normal University, Tianshui 741000, Gansu, China

Abstract: ThiD encoded by *thiD* in *Thermoanaerobacter tengcongensis* is a key enzyme in the biosynthesis of thiamine. The structure and functions of *thiD* have been elucidated in fungi, yeasts, and plants, while the role of *thiD* in thermophiles remains unclear. **[Objective]** This study aims to explore the thermal adaptation mechanism of *T. tengcongensis* and reveal the role of *thiD* in the thermal adaptation of *T. tengcongensis* at different temperatures. **[Methods]** The *thiD*-deleted mutant (Δ*thiD*) of *T. tengcongensis* was constructed by homologous recombination. The growth trends of the wild type (WT) and Δ*thiD* at 50 ℃, 60 ℃, 75 ℃, and 80 ℃ were observed and compared. The differentially expressed genes (DEGs) between Δ*thiD* and WT cultured at 75 ℃ were determined by RNA-seq. The transcript levels of 13 genes and 3 sRNAs in WT and Δ*thiD* at 50 ℃, 60 ℃, 75 ℃, and 80 ℃ were compared and analyzed by real-time PCR. **[Results]** Δ*thiD* was successfully constructed, with the growth rate not significantly different from WT at 50 ℃. However, Δ*thiD* show cased slower growth than WT at 60 ℃ and 75 ℃ and did not grow at 80 ℃. The transcriptome results revealed 503 DEGs in Δ*thiD* compared with WT, including 278 DEGs with up regulated expression and 213 DEGs with down regulated expression. The Kyoto encyclopedia of genes and genomes (KEGG) analysis indicated the following pathways associated with thermophilic adaptation, involving thiamine metabolism, pyrimidine metabolism and purine metabolism, peptidoglycan biosynthesis, fatty acid metabolism, amino acid metabolism, two-component system, DNA replication, homologous recombination, mismatch repair, and phosphotransferase system. The transcript levels of 13 genes and 3 sRNAs related to thermal adaptation in WT and Δ*thiD* changed at specific temperatures. **[Conclusion]** *thiD* plays an important role in the thermal adaptation of *T. tengcongensis*. This study provides experimental data and a theoretical basis for revealing the role of *thiD* in the thermal adaptation of thermophiles at different temperatures.

Keywords: *Thermoanaerobacter tengcongensis*; *thiD*; transcriptome; differentially expressed genes (DEGs); thermal adaptation

✉ actamicro@im.ac.cn, ☎ 010-64807516

Thermophiles are heat-loving microorganisms that thrive in high temperatures above 50 ℃[1]. Numerous attempts have been made to understand the mechanisms of thermal adaptation[2]. However, thermal adaptation is a very complicated process that involves multiple factors. The completion of genome sequences of thermophiles has provided valuable data into the identification of crucial genes involved in thermal adaptation over time[3]. Numerous studies indicated that factors such as the G+C content of the genome and mRNA[4-5], uracil content in 16S rRNA gene[6-8], tRNA modifications[9-11], biosynthesis of fatty acids for energy metabolism[12-13], amino acid composition and utilization[14], as well as thermal adaptation proteins were all associated with thermal adaptation[15]. Furthermore, various temperature-dependent proteins also played important roles in thermal adaptation[16-17].

Thermoanaerobacter tengcongensis was a thermophilic and anaerobic bacterium that was isolated from a hot spring in Tengchong, Yunnan, China. This bacterium could grow from 50 ℃ to 80 ℃, with the optimum growth temperature at 75 ℃[18]. Notably, the genome sequencing and annotation of *T. tengcongensis* were firstly completed in China[3]. The proteomics and genomics related to the thermal adaptation of *T. tengcongensis* have also been studied[19-20]. Genomic analysis showed that a significant proportion (86.7%) of the genes in *T. tengcongensis* were encoded on the leading strand of DNA replication. A strong correlation has been observed between the G+C content of tDNA and rDNA genes and the optimal growth temperature among sequenced thermophiles[3]. Additionally, in the genome of *T. tengcongensis*, glucokinases exhibited thermal stability regulated by their interaction with HSP60[21], while the ribosome recycling factor (tteRRF) demonstrated high thermophilic stability[22]. Transcriptomic analysis has revealed over 1 200 differentially expressed genes (DEGs) in *T. tengcongensis* in response to cold shock, indicating the involvement in various biological processes such as cell wall and membrane remodeling, flagellar assembly, and sporulation[23]. Furthermore, two CRISPR-Cas systems were identified in *T. tengcongensis* that responded to the changes in temperature[24]. The proteomics analysis identified 251 out of 1 589 differentially expressed proteins that exhibited temperature-dependent expression in *T. tengcongensis* at 55, 65, 75 and 80 ℃ using isobaric tags for relative and absolute quantitation[16]. Additionally, 251 temperature-dependent proteins were identified in *T. tengcongensis* by two-dimensional gel electrophoresis and matter-assisted laser desorption/ ionization time-of-flight mass spectrometry at 55, 75, and 80 ℃[25]. *T. tengcongensis* had a phosphoenolpyruvate (PEP) sugar phosphotransferase system (PTS) of 22 proteins[26]. Despite doing these studies, the thermal adaptation mechanisms of *T. tengcongensis* remain unclear.

ThiD is a bifunctional hydroxymethylpyrimidine or methylpyrimidine phosphate kinase, which is a key enzyme in the synthesis of thiamine[27]. Its function is to catalyze the phosphorylation of hydroxymethylpyrimidine (HMP) and hydroxymethylpyrimidine phosphate (HMP-P)[27]. The biochemistry and structure of ThiD have been well studied in most bacteria, yeasts, and plants[28-32]. However, the biological function of ThiD in thermophiles remain unknown. Therefore, in this study, the disruption of *thiD* was constructed to obtain a *thiD* disrupted mutant (Δ*thiD*) and subsequently its role related to the thermal adaptation *T. tengcongensis* was studied. The investigations would deepen our understanding of the thermophilic mechanism of *T. tengcongensis*.

1 Materials and Methods

1.1 Strains and plasmids

T. tengcongensis MB4 (China General Microbiological Culture Collection Centre, deposit number CGMCC 1.2430) was grown in Tris-taurine-EDTA (TTE) medium as described previously[20]. *Escherichia coli* DH5α was cultured in LB medium as described previously[33]. pBOL01 is a shuttle plasmid between *T. tengcongensise* and *E. coli*[20]. pBOL01::Δ*thiD* is a *thiD* disruption plasmid.

1.2 Construction and identification of *thiD* disruption strain

The whole genome of *T. tengcongensis* was isolated by CTAB, and subsequently it was used as a template for PCR amplification of *thiD* left-arm and right-arm fragments with P1 and P2 primers (Table S1). The left arm of *thiD* and plasmid pBOL01 were double digested with *Xho* I and *Hin*d III, and then ligated by T4 DNA ligase and transformed to obtain the recombinant plasmid pBOL01::*thiD* left arm; the left arm of pBOL01::*thiD* recombinant plasmid and the right arm of *thiD* were double enzyme digested with *Bam*H I and *Xba* I, and then the disruption plasmid pBOL01::Δ*thiD* was obtained by ligation and transformation. According to the description of Liu et al[20], 0.1 mL of WT solution was combined with 10 mL of TTE medium at a temperature of 75 ℃ for a duration of 5 hours. Subsequently, 1 mL of this mixture was introduced into another TTE medium along with 50 μL of pBOL01::Δ*thiD* and incubated at 60 ℃ for 3 hours. Following the liquefaction of TTE solid medium and heating to 70 ℃, the above bacterial solution was incorporated into the molten TTE solid medium. This was followed by the addition of 0.5 mL 100 μg/mL kanamycin, thorough mixing, and the transfer of the mixture into anaerobic tubes, which were then flattened and subjected to cultivation at 60 ℃ for a period of 3 to 4 days. Following a single colony grown from the wall of solid anaerobic tubes, individual colonies of Δ*thiD* were selected and propagated in TTE liquid medium supplemented with 0.5 mL of 100 μg/mL kanamycin. The cultures were maintained at a temperature of 60 ℃ for a period of 2 to 3 days until the liquid medium became turbid. Subsequently, the genome was isolated and verified by PCR using primer P3 (Table S1).

1.3 Determination of growth curves of WT and Δ*thiD*

In order to assess the growth of WT and Δ*thiD*, WT and Δ*thiD* were grown respectively at 75 ℃ in 100 mL of TTE medium as described previously[20]. Once the optical density at 600 nm (OD_{600}) of the culture reached 0.6, 1 mL of the culture was transferred to a separate flask containing 100 mL of TTE medium. Subsequently, the culture values at OD_{600} were determined every two hours at 50, 60, 75, and 80 ℃, respectively.

1.4 Total RNA preparation

The WT and Δ*thiD* strains were cultivated in TTE medium at 75 ℃ until an optical density of 0.8 at OD_{600} was achieved. Subsequently, the cells were then collected through centrifugation, and total RNAs were isolated using TRIzol reagent (CWBIO, China). The extracted RNA was further purified with the RNeasy Mini Kit (QIAGEN) and treated with DNase I (RNase-free) (Amboina) to eliminate any potential DNA contamination. The integrity and degradation of the treated RNA were initially assessed using 1% agarose gel electrophoresis. Subsequently, the purity of the RNA was determined using a NanoPhotometer® spectrophotometer, and the concentration was measured using the Qubit® RNA detection kit in a Qubit® 2.0 Fluorimeter. Finally, the RNA integrity was precisely evaluated using the Agilent Technologies 2100 Bio analyzer's RNA Nano 6000 detection kit. The samples with a RIN value above 6 and a concentration exceeding 50 ng/μL were considered to have satisfactory quality.

1.5 RNA-sequencing and analysis of DEGs

Total RNA was used as input material for the RNA sample preparations. A sequencing library was generated using Illumina®'s (NEB) NEBNext®Ultra™ Directional RNA Library Preparation Kit and an index code for the attribute sequence was added to each samples[34]. The library construction was performed following the reference reported by Liu et al.[23]. RNA sequencing was performed by Illumina NovaSeq 6000. Qualified sequences were mapped to the *T. tengcongensis* genome using Bowtie 2-2.2.3 (https://sourceforge.net/projects/bowtie-bio/files/bowtie2/2.2.3/) and paired-end clean reads were aligned to the reference genome using HTSeq v0.6.1[35-36]. The fragments per kilobase of exon model per million mapped fragments (FPKM) of

each gene was calculated using the featureCounts v1.5.0-p3 within the subread software for quantitative assessment[37]. The differential expression analysis of two conditions with three biological replicates per condition, was performed using the DESeq2 R package (1.18.0)[38]. The resulting *P*-values were adjusted using the Benjamini and Hochberg's approach for controlling the false discovery rate[39]. The *P* value<0.05 and |$\log_2$ fold change| value>1 were set as the threshold for significantly differential expression[40].

The gene ontology (GO) enrichment analysis of DEGs was implemented by the cluster Profiler R package (3.8.1), and gene length bias was corrected[41]. KOBAS was used to test the statistical enrichment of DEGs in KEGG pathways[42]. The Diamond software (0.9.13) was utilized to compare the target gene sequences with the selected reference[43], and then the network was established based on the known interaction of the selected reference species. The protein interactions of 141 DGEs in 30 KEGG pathways were analyzed by STRING (https://www.string-db.org/). Cytoscape (3.9.1) (https://Cytoscape.org/) was used to screen out central DEGs to the protein-protein interaction (PPI) networks[44]. In the PPI networks, the FPKM of DEGs with a selection degree greater than 10 was used as the expression level to generate heatmaps. The FPKM value of differential genes of different strains was taken as the expression level to do hierarchical cluster analysis. Different colors represent different clustering information. Genes within the same group exhibited similar expression patterns, suggesting potential functional similarities or involvement in the same biological process. The lg (FPKM+1) values were normalized and clustered, with red indicating high-expression genes and blue indicating low-expression genes.

1.6 Real-time PCR

cDNA was synthesized from each RNA sample using the TransScript® All-in-One First-Strand cDNA Synthesis SuperMix (Transgen Biotech Co., Ltd, Beijing). The primers used for real-time PCR are listed in Table S1. The relative expression values of WT in *thiD* were assigned as 1 with the 16S rRNA gene used as a reference. All samples were analyzed in triplicate, and the data were processed using Light Cycler® 96 software (version 1.1.0.1320), each reaction volume was 20 μL, and the relative expression values of the genes were calculated using the $2^{-\Delta\Delta C_t}$ method and the normalization method. The results were represented as means ± standard errors (SD)[23]. The expression levels of 12 genes and 3 sRNAs associated with the thermal adaptation mechanism in the Δ*thiD* were assessed at temperatures of 50 ℃, 60 ℃, and 75 ℃ using real-time PCR. GraphPad Prism 8 software was employed for data analysis.

2 Results

2.1 Construction and identification of *thiD* disruption strain

The PCR analysis demonstrated that both 1 108 bp *thiD* right arm and left arm were obtained (Figure 1A). The recombinant plasmid pBOL01::*thiD* left arm was successfully constructed (Figure 1B). By double enzyme digestion of recombinant plasmids pBOL01::Δ*thiD*, 5 000 bp and 1 108 bp fragments were obtained (Figure 1C). The genome extracted from the Δ*thiD* strain was used as a template to amplify and obtained a 3 200 bp fragment, and the genome of the WT strain was used as a template to amplify and obtained a 2 800 bp fragment (Figure 1D). This indicated that the *thiD* disruption strain was successfully constructed.

2.2 Determination of growth curves of WT and Δ*thiD*

The growth rate of Δ*thiD* was not significantly different from that of the wild type (WT) strain at 50 ℃ (Figure 2A). Nevertheless, the growth rate of Δ*thiD* was significantly slower in comparison with the WT strain at 60 ℃ and 75 ℃ (Figure 2B, 2C). Obviously, Δ*thiD* almost did not grow at 80 ℃ (Figure 2D).

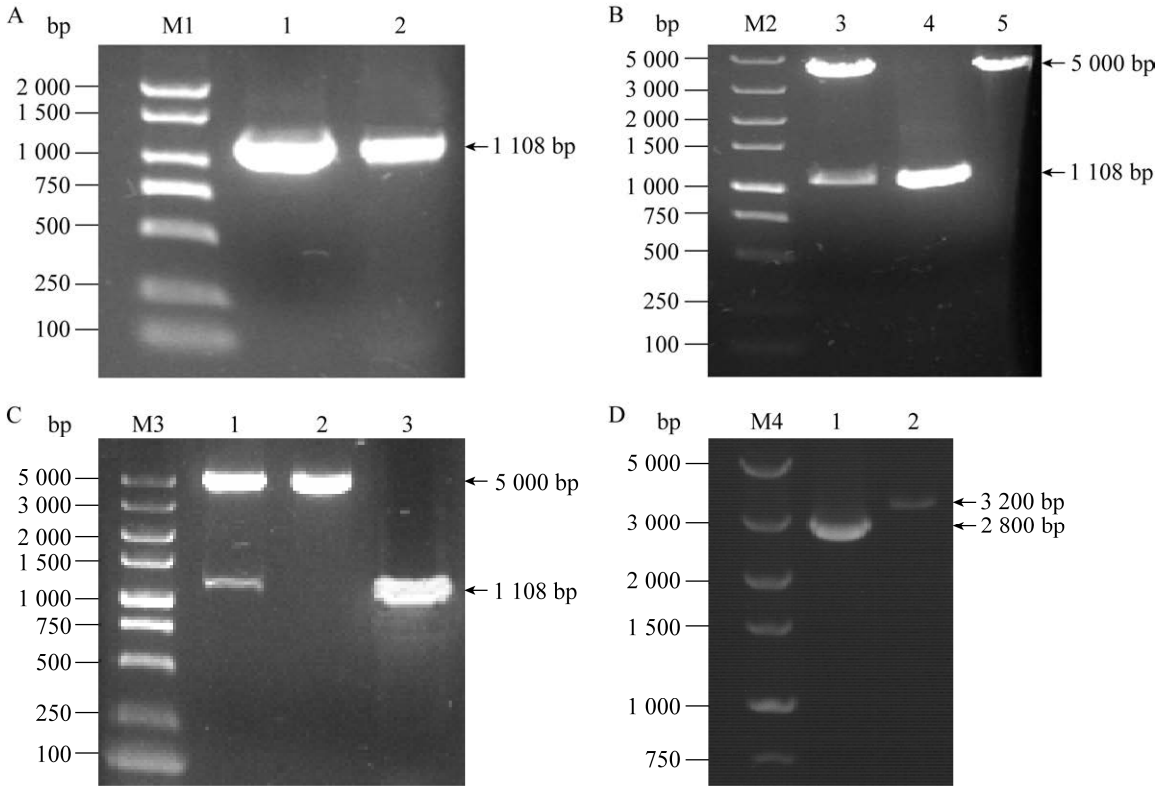

Figure 1 PCR verification of Δ*thiD*. A: PCR amplification of left and right arm of *thiD*. M1: DL2000 Plus DNA Marker. 1: Left arm of *thiD*; 2: Right arm of *thiD*. B: Endonuclease digestion identification of recombinant plasmid. M2: DL5000 DNA Marker; 3: Endonuclease digestion products of pBOL01::right arm of *thiD* digested with *Xho* I and *Hin*d III; 4: Left arm *thiD* digested with *Xho* I and *Hin*d III; 5: Endonuclease digestion products of pBOL01 digested with *Xho* I and *Hin*d III. C: Endonuclease digestion identification recombinant plasmids pBOL01::Δ*thiD*. M3: DL5000 DNA Marker; 1: Endonuclease digestion products of pBOL01::Δ*thiD* digested with *Bam*H I and *Xba* I; 2: Endonuclease digestion products of pBOL01::left arm of *thiD* digested with *Bam*H I and *Xba* I; 3: *thiD* right arm PCR fragment. D: PCR identification of Δ*thiD*. M4: DL5000 DNA Marker. 1: PCR amplification of WT genome as template; 2: PCR amplification using Δ*thiD* as template.

2.3 Transcriptome analysis of WT and Δ*thiD* strains

In this study, we selected differentially expressed genes through two levels of multiple of difference ($|\log_2$ fold change$|>1$) and significance level ($P<0.05$) by DESeq2. By comparing the gene expression of the Δ*thiD* strain at 75 ℃ with that of the WT strain, a total of 503 DEGs were identified, by which consisted of 278 up regulated DEGs and 213 down regulated DEGs (Figure 3A, Table S2).

The top 10 up regulated and down regulated genes are listed in Table 1. Among the most up regulated genes, *tte1563* encoded the enzyme related to GTP cyclohydrolase I and *thiM* was a gene encoding hydroxyethylthiazole kinase.

The GO analysis revealed that there were 1 086 up regulated GO terms and 1 251 down regulated GO terms. The specific details are provided in table S3. The top 25 enrichment groups were evaluated based on their *P* values within the GO categories of biological process, cellular component, and molecular function, as depicted in Figure 3B. Noteworthy subcategories included carbohydrate derivative metabolic process, nucleobase-containing small molecule metabolic

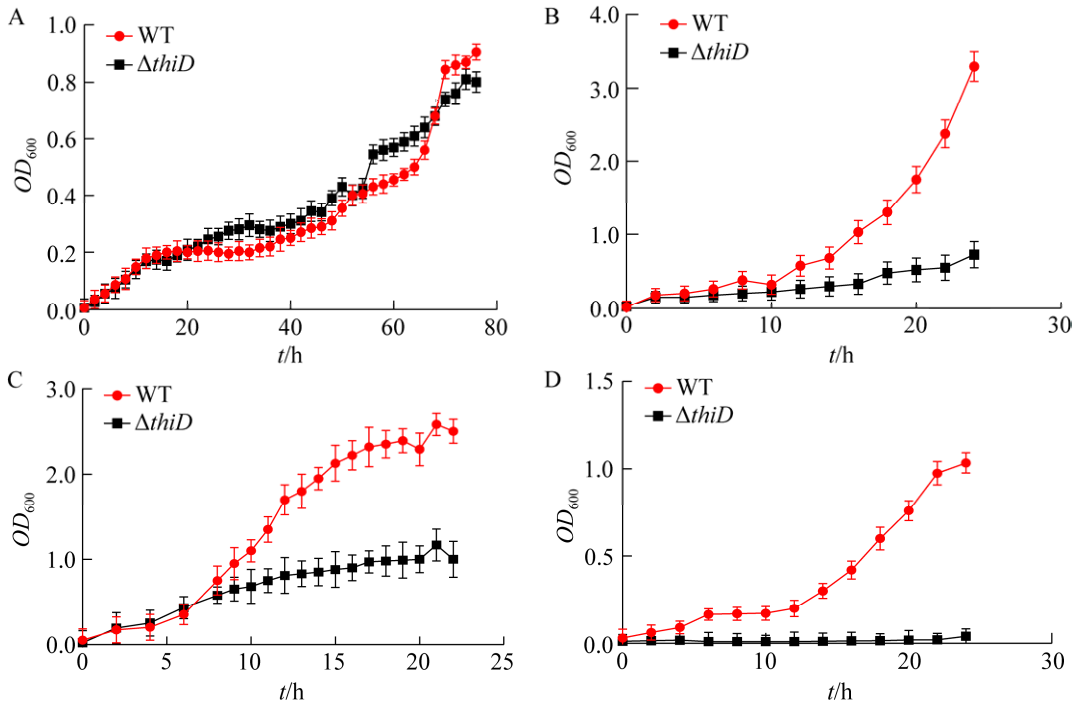

Figure 2 The growth curves of Δ*thiD* and WT at different temperatures. A: The growth curves of Δ*thiD* and WT at 50 ℃. B: The growth curves of Δ*thiD* and WT at 60 ℃. C: The growth curves of Δ*thiD* and WT at 75 ℃. D: The growth curves of Δ*thiD* and WT at 80 ℃.

process, and nucleoside phosphate metabolic process. Nucleotide metabolic process, tetrapyrrole metabolic process, and ribose phosphate metabolic process were prominently represented. These results indicated that the DEGs of these processes were all involved in the process of thermal adaptation.

The analysis of enriched KEGG revealed that there were 96 pathways, with specific details provided in Table S4. Among these pathways, 30 important pathways related to thermal adaptation were further screened out. As shown in Figure 3C, the metabolic pathway was the largest number of annotation pathway. Additionally, the TCS, ribosome, 2-oxo-carboxylic acid metabolism, PTS, degradation of valine, leucine and isoleucine, homologous recombination, and mismatch repair pathways were related to thermal adaptation.

Furthermore, the PPI networks were constructed using 141 DEGs derived from 30 signaling pathways, including up regulated 77 DEGs and 64 down regulated DEGs. The protein interactions of 141 DGEs in 30 KEGG pathways were analyzed using STRING. According to Cytoscape program, 91 interacting proteins of DEGs in the PPI networks were identified. The key DEGs ranked by gene degree included *tal*, *pgi*, *atp*F, *atp*H, *aro*K, *aro*B, ANT_16660, ANT_13390, *atp*A, *dna*N, and *nuo*G (Figure 3D). Subsequently, DEGs with a degree greater than 10 were selected, and their FPKM values were used to generate heatmaps. The heatmap consisted of 36 DEGs (19 up regulated and 17 down regulated DEGs) (Figure 3E). The *pgi* was involved in carbon metabolism pathway, while *atpF* and *atpH* were associated with in oxidative phosphorylation pathway. Additionally, the *aroK* and *atpA* participated in metabolic pathways, and DNA polymerase III beta subunit (*dnaN*) participated in the citrate cycle.

To thoroughly examine the expression of genes identified in the RNA-seq analysis, we performed real-time PCR on three of the most highly expressed genes (*thiE*, *tte0003*, and *napF3*), three of the most up regulated genes

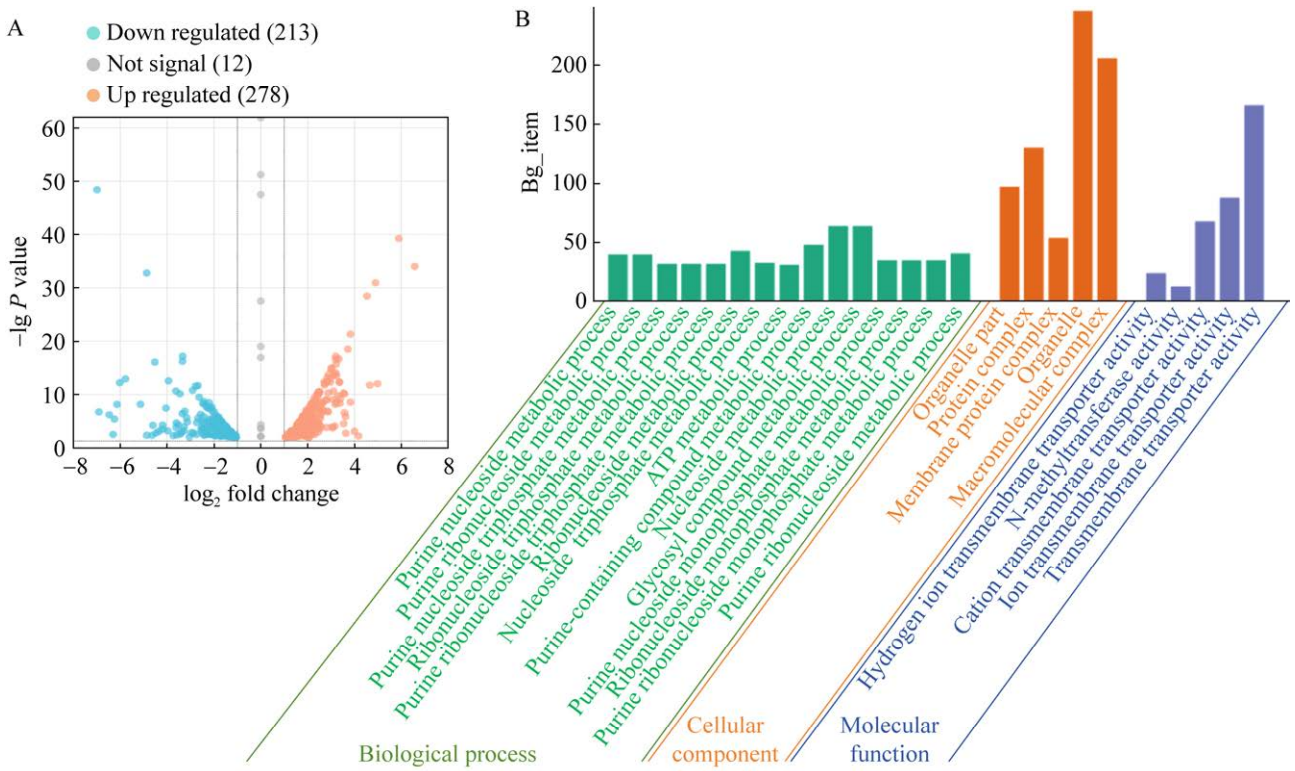
A
Down regulated (213)
Not signal (12)
Up regulated (278)
−lg P value
log2 fold change
B
Bg_item
Purine nucleoside metabolic process
Purine ribonucleoside metabolic process
Nucleoside triphosphate metabolic process
Ribonucleoside triphosphate metabolic process
Purine ribonucleoside triphosphate metabolic process
Nucleoside triphosphate metabolic process
Purine-containing compound metabolic process
Glycosyl compound metabolic process
Nucleoside monophosphate metabolic process
Ribonucleoside monophosphate metabolic process
Purine ribonucleoside monophosphate metabolic process
Organelle part
Protein complex
Membrane protein complex
Organelle
Macromolecular complex
Hydrogen ion transmembrane transporter activity
N-methyltransferase activity
Cation transmembrane transporter activity
Ion transmembrane transporter activity
Transmembrane transporter activity
Biological process
Cellular component
Molecular function

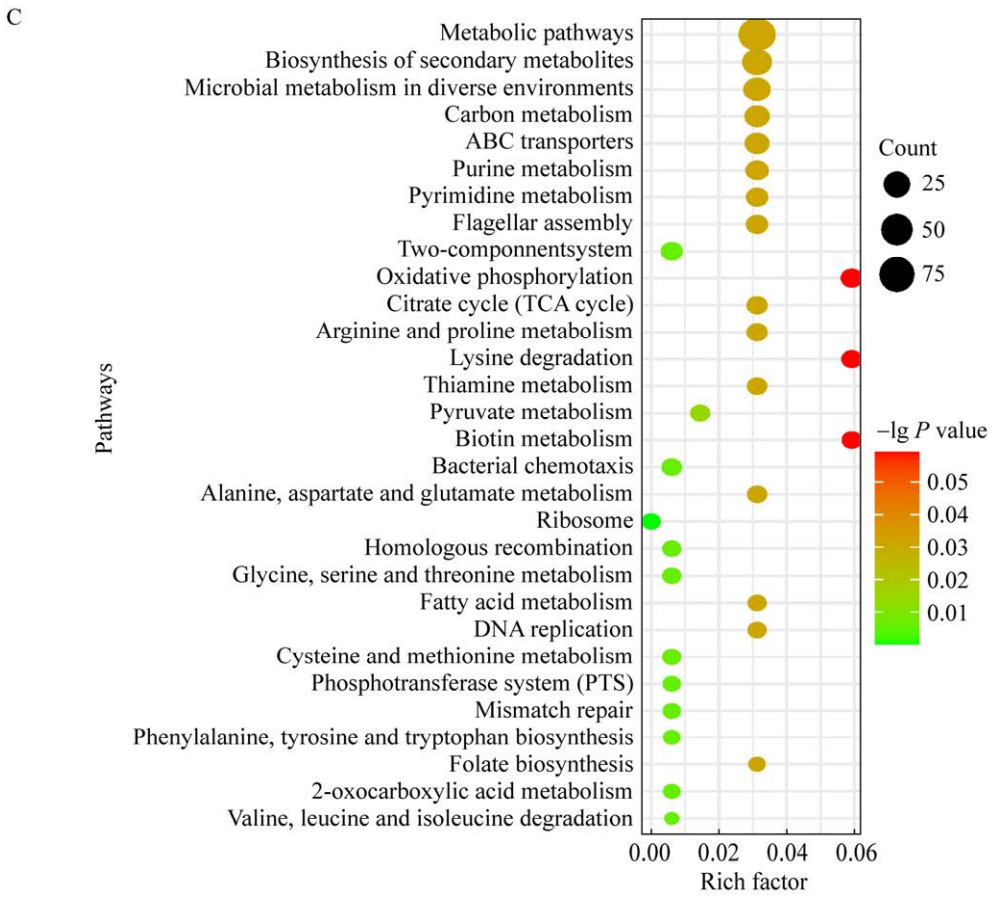
C
Metabolic pathways
Biosynthesis of secondary metabolites
Microbial metabolism in diverse environments
Carbon metabolism
ABC transporters
Purine metabolism
Pyrimidine metabolism
Flagellar assembly
Two-componnentsystem
Oxidative phosphorylation
Citrate cycle (TCA cycle)
Arginine and proline metabolism
Lysine degradation
Thiamine metabolism
Pyruvate metabolism
Biotin metabolism
Bacterial chemotaxis
Alanine, aspartate and glutamate metabolism
Ribosome
Homologous recombination
Glycine, serine and threonine metabolism
Fatty acid metabolism
DNA replication
Cysteine and methionine metabolism
Phosphotransferase system (PTS)
Mismatch repair
Phenylalanine, tyrosine and tryptophan biosynthesis
Folate biosynthesis
2-oxocarboxylic acid metabolism
Valine, leucine and isoleucine degradation
Pathways
Rich factor
Count
−lg P value

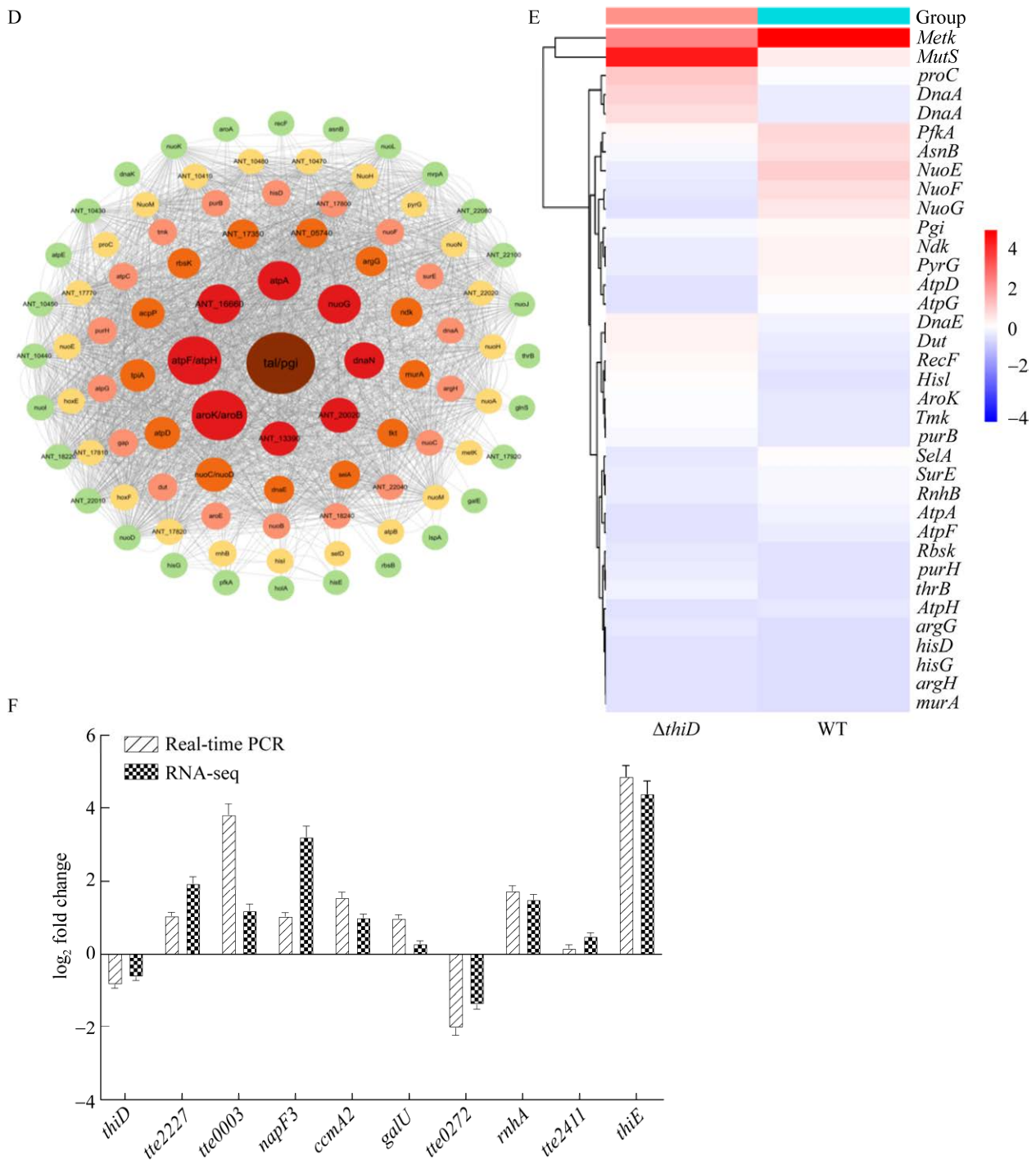

Figure 3 Transcriptome data analysis. A: Volcano plot of total DEGs in Δ*thiD* compared with WT groups. Red plots represent up regulated DEGs, and blue plots represent down regulated DEGs. B: GO functional enrichment pathway of DEGs in the top 25 enrichment groups. C: KEGG enrichment analysis of selected DEGs in thirty important pathways. D: The PPI networks of selected DEGs. E: Clustering diagram of important DEGs. Red represents highly DEGs and blue represents lowly DEGs. F: Validation of DEGs by real-time PCR. Comparison of RNA-seq and real-time PCR measures of changes in the expression of *thiD*, *tte2227*, *tte0003*, *napF3*, *ccmA2*, *galU*, *tte0272*, *rnhA*, *tte2411*, and *thiE*.

(*tte2227*, *ccmA2*, and *rnhA*), two of the most down regulated genes (*tte0272* and *thiD*), and two moderately repressed genes (*galU* and *tte2411*). The results from the real-time PCR were basically consistent with the transcriptome data, indicating that the transcriptome sequencing results had high reliability and could be used as a reference for bioinformatics (Figure 3F).

2.4 The expression of specific DEGs in Δ*thiD* at different temperatures

Using the real-time PCR, Δ*thiD* was compared with WT at 50, 60, 75 and 80 ℃ and the specific genes mentioned below were obtained. The expression of *tte2227* at 50 ℃ was significantly lower than that of WT, while significantly higher at 60 ℃ (Figure 4B−4C). The *thiE* identified as a thiamine phosphate synthetase gene displayed higher expression levels than WT at 50, 60, 75 and 80 ℃, with the highest expression observed at 80 ℃ (Figure 4A−4D). In contrast, the *thiD*, a gene encoding a bifunctional hydroxymethylpyrimidine or methylpyrimidine phosphokinase, showed no expression at 50, 60, and 75 ℃ in comparison with that of WT, but exhibited increased expression at 80 ℃ when compared with that at 50 ℃ (Figure 4A−4D). Furthermore, the *tte0620* was basically not expressed at 50 ℃ and 60 ℃, but was higher than WT at 75 ℃ (Figure 4B−4D). Similarly, the *tte0003* was not expressed at 50 ℃, but was significantly higher than WT at 60 ℃ and 75 ℃ (Figure 4B−4D). Conversely, the expression levels of *tte0272*, *rnhA* and *napF3* were significantly lower than those of WT at 50 ℃, but increased at 60 ℃ and 75 ℃ (Figure 4B−4D). On the other hand, only the *ccmA2* and *tte2763* exhibited significantly higher expression levels than WT at 60 ℃, while the *ccmA2*, *tte2763*, and *tte2411* displayed significantly higher expression levels than WT at 75 ℃ (Figure 4C−4D). Furthermore, the *tte2411* was not expressed at 50 ℃ and 60 ℃, but was significantly higher than WT at 75 ℃ (Figure 4B−4D). In addition, non-coding RNAs such as sRNA49, sRNA103, and sRNA104 exhibited different expression levels compared to WT at specific temperatures.

Table 1 The largest change of top ten up regulated and down regulated genes

Rank	Gene	$\log_2$ fold change	Annotation
1↑	*tte1563*	Infinity	Enzyme related to GTP cyclohydrolase I
2↑	sRNA00086	6.574 1	Unknown
3↑	*thiM*	5.894 4	Hydroxyethylthiazole kinase, sugar kinase family
4↑	*tte2506*	4.981 7	Hypothetical protein
5↑	*thiE*	4.897 6	Thiamine monophosphate synthase
6↑	*tte0230*	4.650 1	Hypothetical protein
7↑	*fabG5*	4.535 2	Dehydrogenases with different specificities (related to short-chain alcohol dehydrogenases)
8↑	*rpmI*	4.176 2	Ribosomal protein L35
9↑	*tte1519*	3.996 0	Hypothetical protein
10↑	*ptsN3*	3.829 0	Phosphotransferase system mannitol/fructose-specific IIA domain (Ntr-type)
1↓	*tte0239*	−Infinity	Transposase
2↓	*atpB*	−Infinity	F0F1-type ATP synthase a subunit
3↓	*atpE*	−Infinity	F0F1-type ATP synthase c subunit/Archaeal/vacuolar-type H^+-ATPase subunit K
4↓	*atpF*	−Infinity	F0F1-type ATP synthase b subunit
5↓	*atpH*	−Infinity	F0F1-type ATP synthase delta subunit
6↓	*atpA*	−Infinity	F0F1-type ATP synthase alpha subunit
7↓	*atpG*	−Infinity	F0F1-type ATP synthase gamma subunit
8↓	*atpD*	−Infinity	F0F1-type ATP synthase beta subunit
9↓	*tte0854*	−Infinity	Hypothetical protein
10↓	*tte1171*	−Infinity	Hransposase

↑: Up; ↓: Down; −: Negative number.

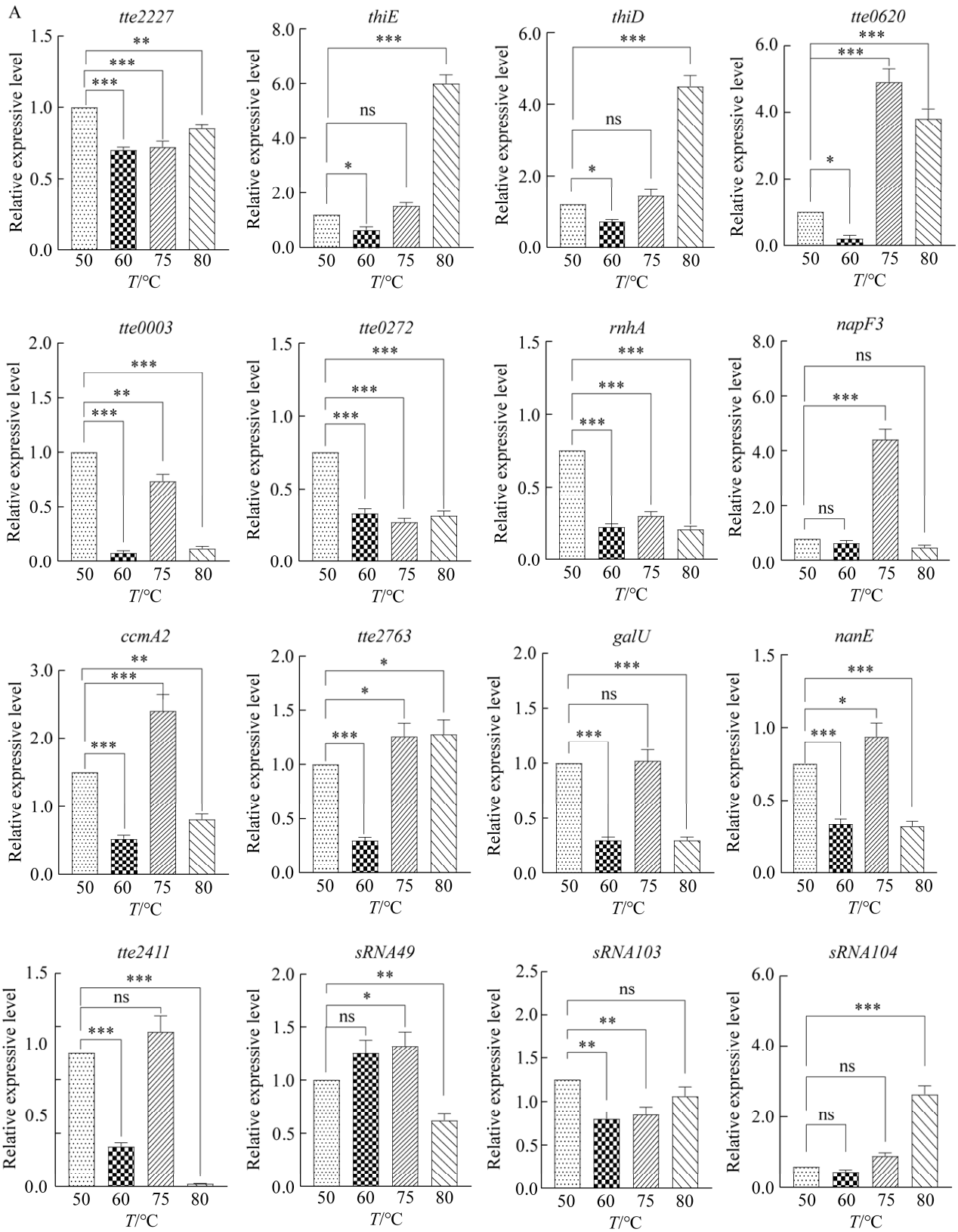
A
tte2227
thiE
thiD
tte0620
tte0003
tte0272
rnhA
napF3
ccmA2
tte2763
galU
nanE
tte2411
sRNA49
sRNA103
sRNA104
Relative expressive level
T/°C
50
60
75
80
ns
*
**
***

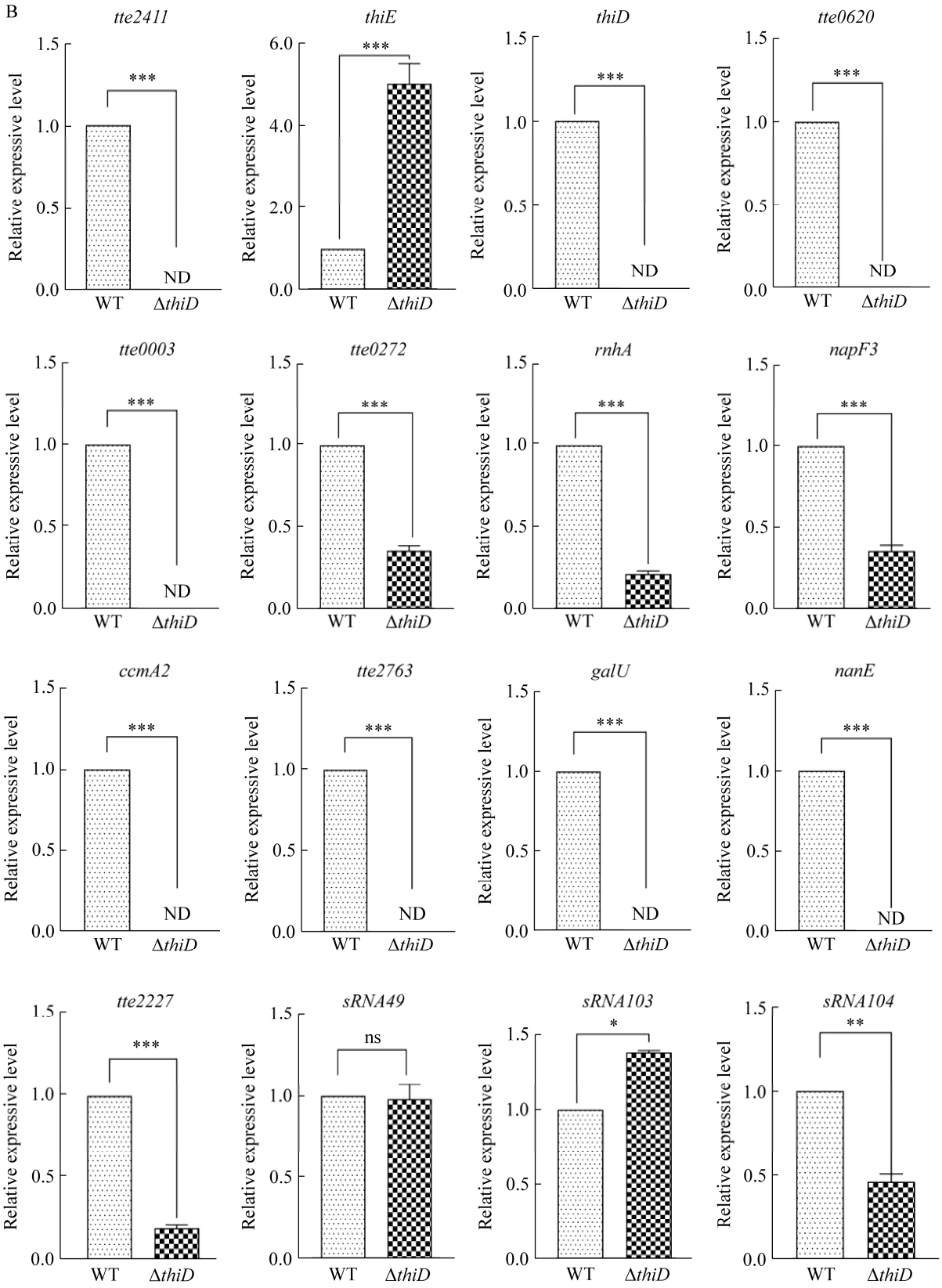
B
tte2411
thiE
thiD
tte0620
tte0003
tte0272
rnhA
napF3
ccmA2
tte2763
galU
nanE
tte2227
sRNA49
sRNA103
sRNA104
Relative expressive level
***
*
**
ns
ND
WT
ΔthiD

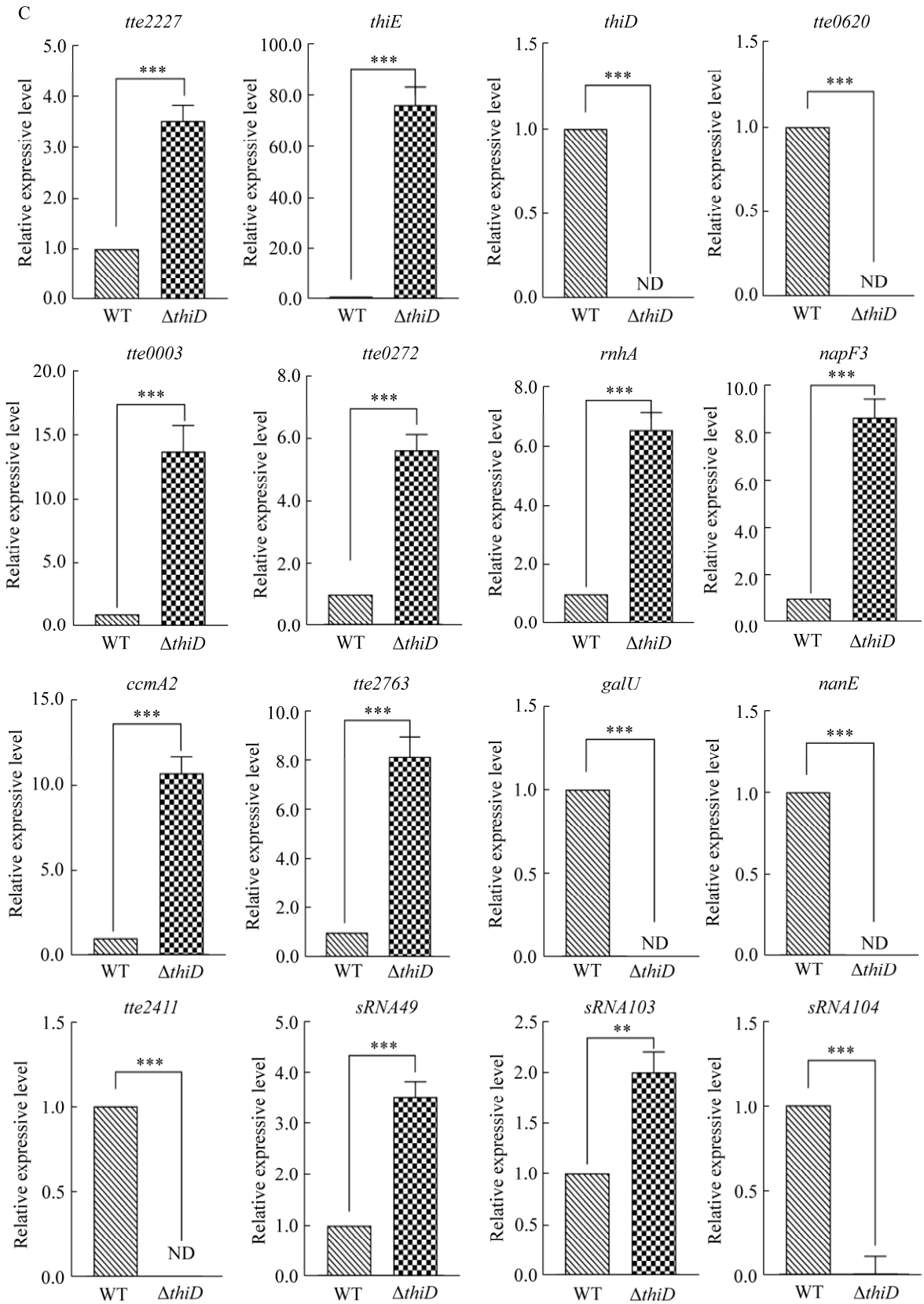
C
tte2227
thiE
thiD
tte0620
tte0003
tte0272
rnhA
napF3
ccmA2
tte2763
galU
nanE
tte2411
sRNA49
sRNA103
sRNA104
Relative expressive level
WT
ΔthiD
ND
***
**

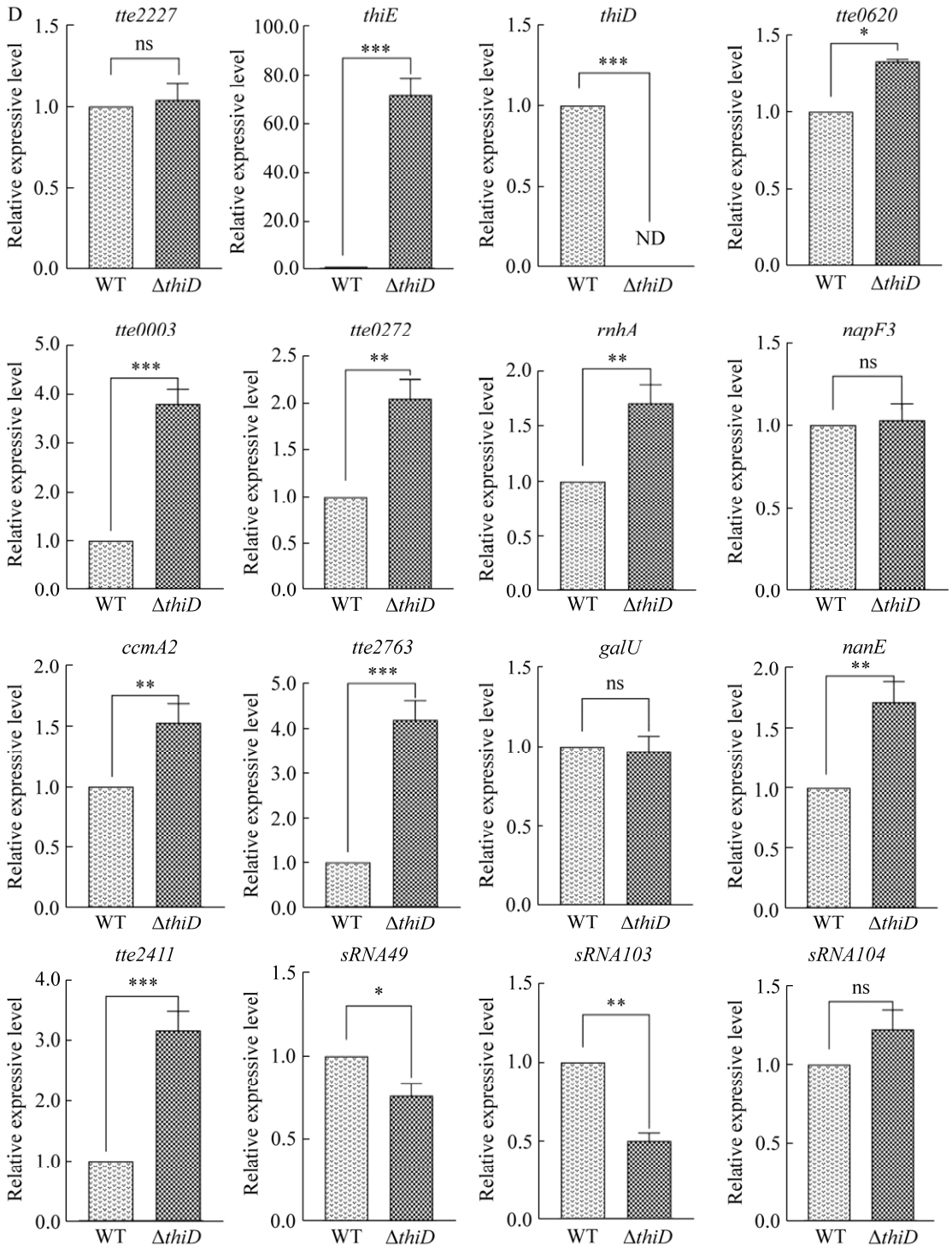

Figure 4 The expression analysis of Δ*thiD* specific gene by real-time RCR. A: The expression analysis of WT specific genes by real-time PCR at 50, 60, 75 and 80 ℃. The expression level in the samples of WT at 50 ℃ was set as 1). B, C, D: The expression analysis of specific DEGs of of WT and Δ*thiD* 50 ℃, 60 ℃, 75 ℃ by real-time RCR, respectively. The expression level in WT was set as 1, ND: No detection. *: Represents the difference within experimental groups; *: $P<0.05$; **: $P<0.01$; ***: $P<0.001$; Error bars in graphs represent standard errors. ns: No significant difference.

3 Discussion and Conclusions

In this study, the *thiD* disrupted mutant did not grow at 80 ℃, and the growth rate at 50, 60 and 75 ℃ was slower than that of the WT strain, indicating that *thiD* played a role in the normal growth, metabolism, and survival of *T. tengcongensis*. Based on the transcriptome analysis, we suggested that high-temperature growth of *T. tengcongensis* was mainly associated with the expression of genes related to thiamine biosynthesis pathways, purine and pyrimidine metabolism, peptidoglycan biosynthesis, fatty acid biosynthesis, amino acid metabolism, TCS, DNA replication, recombination and repair, the ribosomal pathway, PTS, the central carbon metabolism, glycolysis, pentose phosphate pathway, tricarboxylic acid cycle, and glycolysis.

3.1 Biological roles of *thiD* and *thiE*

Thiamine pyrophosphateas a cofactor for several enzymes were essential for the metabolism of carbohydrates and amino acids[27]. In bacterial genomes, genes encoding enzymes were involved in thiamine biosynthesis pathways, such as the *thiD*, *thiE*, and *thiM*, as the key genes in thiamine metabolism and 2-oxo carboxylic acid metabolism. In *T. tengcongensis*, *the thiD* regulated the thiamine metabolic pathway by encoding a dipyromethylpyrimidine phosphokinase and catalyzing the phosphorylation of HMP and HMP-P to adapt to high temperature[28]. And the expression levels of *thiD* at 50 ℃ and 60 ℃ and 75 ℃ were consistent with the trend of the analysis at different temperatures by Wang et al.[24]. Other genes involved in thiamine metabolism included the *thiE*, which was the thiamine phosphate synthetase gene. And the deletion of *thiD* resulted in the increased expression and up-regulation of other genes involved in thiamine metabolism including the *thiE*, *thiM*, *thi80*, and *nifS2*, which ensured the stable growth of Δ*thiD* at different temperatures.

3.2 DEGs involved in purine metabolism and pyrimidine metabolism

The involvement of DGEs in purine and pyrimidine metabolism suggested that the key to maintaining thermophilic stability of *T. tengcongensis* at extreme growth temperatures was fundamentally dependent on the stability of genetic material. The high content and frequency distribution of guanine and cytosine in genetic material significantly enhanced the stability of proteins[45]. In this study, purine metabolism demonstrated the upregulation of eight DEGs (*nrdA*, *dnaN*, *purB*, *dnaE*, *purC*, *purM*, *purN*, and *purH*) and pyrimidine metabolism showed the upregulation of five DEGs (*dnaN*, *tmk*, *dut*, *nrdA*, and *dnaE*). The results suggested that, in terms of nucleotide composition, the relative abundance of purines, particularly the increased frequency of adenine, in the coding sequences of thermophiles might contribute to genetic material stability by stabilizing the tertiary structure[9]. In addition, other mechanisms such as modifications of rRNA, tRNAs, selective translation of codon-biased transcripts, and regulation of translation elongation were also considered as the positive ways to respond to environmental changes[46-49].

3.3 DEGs involved in cell wall and membrane structures

Peptidoglycan biosynthesis was a crucial process in the formation of bacterial cell walls, serving as the main structural component and provided protection against environmental stress in various organisms[50]. In this study, the expression of *pgi* encoding glucose-6-phosphate isomerase, which is involved in glycolysis, fructose-6-phosphate and UDP-N-acetylglucosamine biosynthesis, was up regulated. UDP-N-acetylglucosamine was an essential component and precursor of bacterial peptidoglycan[51-52]. The up-regulation of the *pgi* implied that these pathways provided essential energy and precursor molecules for the metabolism of *T. tengcongensis*. Furthermore, the enhanced biosynthesis and accumulation of peptidoglycan were responsible for protecting the cell integrity of *T. tengcongensis* against temperature fluctuations.

Moreover, the fatty acid biosynthesis pathway could modulate the response of the cell membrane of thermophiles to different temperatures

by altering branched-chain fatty acid content and controlling the biophysical properties of membrane phospholipids enabling them to survive in extreme environments[12]. The results indicated that fatty acid and phospholipid biosynthesis enzyme phosphoacyltransferase (*plsX*) were involved in the formation of fatty acid and phospholipid, indicating that *T. tengcongensis* modified the original phospholipid structure during the process of thermal adaptation[50]. This process involved precise adjustments to the composition of membrane lipids to maintain the necessary fluidity of cell membranes at different temperatures.

3.4 DEGs involved in amino acid metabolic pathways

Regulating the metabolism of amino acids has been identified as a potentially effective strategy for protecting cells from the adverse effects of temperature variations[53]. This study revealed that the expressions of lysine, glutamate, valine, isoleucine, and tyrosine were up regulated, whereas alanine, histidine, glutamine, and threonine, were down regulated. By regulating the metabolic pathway of arginine and proline, and upregulating the degradation pathway of lysine, it would be possible to enhance the production of thermal adaptive proteins[54]. This study indicated that significant alterations in the levels of these amino acids played a role in enhancing the thermal stability of proteins.

3.5 DEGs involved in two-component regulation

A two-component system was regarded as a common signaling pathway in many bacteria, serving as information processing pathways that linked external stimuli with adaptive responses within cells. In prokaryotes, signal transduction was mainly carried out by a two-component regulatory system[55-56]. The two-component system was responsible for cellular responses to diverse environmental stimuli, effectively regulating gene expression[57]. In this study, the up regulated *cheY2* expression was consistent with the trend of RNA-sequencing analysis of cold shock response in *T. tengcongensis*, a bacterium harboring a single cold shock protein encoding gene reported by Liu et al.[23]. In addition, the expression patterns of *cheY7* at 80 ℃, as well as the *baeS12* and *ompR4* at 50 ℃ in *T. tengcongensis*, was consistent with the results found by Wang et al.[24]. *T. tengcongensis* had a typical two-component system consists of two key elements: histidine kinases sensory transduction (*ddpX* and *baeS12*), which are sensitive to a specific environmental factor, and a response regulator *ompR4*, facilitating the transmission of the sensor signals and adapting the proper responses *via* the regulation of gene expression. These components play a key role in two typical two-component systems that transmit sensor signals and modulate gene expression to elicit suitable responses[58]. This study indicates that the signal DEGs associated with this pathway in signal transduction plays a significant role in participating in the thermal adaptation mechanism of *T. tengcongensis*.

3.6 DEGs involved in DNA replication, recombination and repair

Three interconnected biological processes, specifically DNA replication, recombination, and repair, were essential for maintaining the fidelity and integrity of the genome[59]. This study focused on analyzing the expression of DEGs associated with thermal adaptation of *T. tengcongensis* in DNA replication, mismatch repair and homologous recombination. Among them, the *dnaE*, *dnaN* and *holB* participated in low temperature induction. Additionally, the *rnhB* was associated with *oriC*-dependent chromosome replication, while the product of *recF* functioned as a recombinational DNA repair ATPase, serving multiple roles in DNA repair, homologous gene recombination, and DNA replication[60]. And the *mutS* was responsible for mismatch repair[61]. The upregulation of *DnaN* and *DnaE* encoding the chromosome replication initiation proteins at the mRNA level was observed, while the expression of *RnhB* and *HolA* was down regulated. Furthermore, the single-stranded DNA-binding protein SSB

also played a crucial role in DNA replication, recombination, and damage repair processes[62]. These results suggested that the biological processes could enable *T. tengcongensis* to survive at extreme temperatures by adapting to ambient temperature[63].

Additionally, the *rpmI*, a gene involved in the ribosomal pathway, has been related to the thermotropism of *T. tengcongensis*[64]. The *ptsN3* encoding the mannitol/fructose-specific IIA structural domain of the phosphotransferase system (Ntr-type) exhibited a significant upregulation in transcript levels during thermophilic acclimatization, indicating its crucial involvement in the PTS[65]. The primary energy source for the organism was typically derived from central carbon metabolism, which encompassed glycolysis, the TCA cycle, and the pentose phosphate pathway, providing essential precursor materials for other metabolic pathways[66].

3.7 Induction of novel DEGs and DEGs with unknown function

In this study, a total of 16 specific DEGs were identified at 50, 60, 75, and 80 ℃. Among these, the ferritin gene *napF3*, which was involved in membrane lipid synthesis, also played an important role in different signaling pathways[3,21]. The *rnhA* was a ribonuclease HI gene associated with mouth-dependent chromosome replication[67]. Furthermore, the *ccmA2*, a gene encoding a multidrug ABC transporter ATPase, was crucial for maintaining the normal morphology of bacteria and was closely related to the operation of bacteria[68]. In addition, sRNA49, sRNA103, and sRNA104 were small RNAs that had the potential to modulate the expression of proteins related to thermophiles proteins[69]. However, the names and functions of the remaining genes are unknown, and their regulatory mechanisms of thermal adaptation in thermophiles also remain unclear. These results suggested that these DEGs might interact with *thiD* at different temperature, thereby influencing the activity of Δ*thiD* and assuming other physiological functions in the process of thermal adaptation.

In conclusion, the *thiD* disrupted mutant did not grow at 80 ℃, and its growth rate at 50, 60, and 75 ℃ was slower than that of the WT strain, indicating that ThiD played a role in the normal growth, metabolism, and survival of *T. tengcongensis*. The transcriptome analyses indicated that the thermal adaptation of *T. tengcongensis* involved the coordinated regulation of various signaling pathways. It was observed that only a limited set of DEGs within each pathway were modified and involved in the regulation of thermal adaptation. However, additional empirical evidence is necessary to comprehensively elucidate *T. tengcongensis* to thrive in high-temperature environments. This study would provide new insights into the mechanisms of thermal adaptation in *T. tengcongensis*.

Supplementary Materials

The following supporting information can be downloaded at: Table S1: The oligonucleotide sequences used in this experiment. Table S2: Differentially expressed genes according to DESeq analysis. Table S3: All GO functional pathway of Δ*thiD* compared with WT groups. Table S4: All KEGG analysis of DEGs in Δ*thiD* compared with WT groups. (Schedule 1, data submitted to National Microbiology Science Data Center, number: NMDCX0000290)

Data Availability Statement

The datasets generated during the current study are available in the [NCBI BioProject] repository [https://www.ncbi.nlm.nih.gov/sra/PRJNA1030901. The accession number is PRJNA1030901].

Acknowledgments

We thank Professor Huarong Tan (The Institute of Microbiology, Chinese Academy of Sciences, Beijing) for providing the *Thermoanaerobacter tengcongensis* MB4 strain.

Conflicts of Interest

The authors declare no conflict of interest.

References

[1] WANG XW, TAN X, DANG CC, LU Y, XIE GJ, LIU BF. Thermophilic microorganisms involved in the nitrogen cycle in thermal environments: advances and prospects[J]. Science of the Total Environment, 2023, 896: 165259.

[2] LÓPEZ-ORTEGA MA, CHAVARRÍA-HERNÁNDEZ N, LÓPEZ-CUELLAR MDR, RODRÍGUEZ-HERNÁNDEZ AI. A review of extracellular polysaccharides from extreme niches: an emerging natural source for the biotechnology. from the adverse to diverse[J]. International Journal of Biological Macromolecules, 2021, 177: 559-577.

[3] BAO QY, TIAN YQ, LI W, XU ZY, XUAN ZY, HU SN, DONG W, YANG J, CHEN YJ, XUE YF, XU Y, LAI XQ, HUANG L, DONG XZ, MA YH, LING LJ, TAN HR, CHEN RS, WANG J, YU J, YANG HM. A complete sequence of the *T. tengcongensis* genome[J]. Genome Research, 2002, 12(5): 689-700.

[4] TENG WK, LIAO B, CHEN MY, SHU WS. Genomic legacies of ancient adaptation illuminate GC-content evolution in bacteria[J]. Microbiology Spectrum, 2023, 11(1): e0214522.

[5] HU EZ, LAN XR, LIU ZL, GAO J, NIU DK. A positive correlation between GC content and growth temperature in prokaryotes[J]. BMC Genomics, 2022, 23(1): 110.

[6] KHACHANE AN, TIMMIS KN, DOS SANTOS VAPM. Uracil content of 16S rRNA of thermophilic and psychrophilic prokaryotes correlates inversely with their optimal growth temperatures[J]. Nucleic Acids Research, 2005, 33(13): 4016-4022.

[7] JAY ZJ, INSKEEP WP. The distribution, diversity, and importance of 16S rRNA gene introns in the order *Thermoproteales*[J]. Biology Direct, 2015, 10: 35.

[8] MIYAZAKI K, TOMARIGUCHI N. Occurrence of randomly recombined functional 16S rRNA genes in *Thermus thermophilus* suggests genetic interoperability and promiscuity of bacterial 16S rRNAs[J]. Scientific Reports, 2019, 9: 11233.

[9] LORENZ C, LÜNSE CE, MÖRL M. tRNA modifications: impact on structure and thermal adaptation[J]. Biomolecules, 2017, 7(2): 35.

[10] OHIRA T, MINOWA K, SUGIYAMA K, YAMASHITA S, SAKAGUCHI Y, MIYAUCHI K, NOGUCHI R, KANEKO A, ORITA I, FUKUI T, TOMITA K, SUZUKI T. Reversible RNA phosphorylation stabilizes tRNA for cellular thermotolerance[J]. Nature, 2022, 605: 372-379.

[11] HORI H. Regulatory factors for tRNA modifications in extreme- thermophilic bacterium *Thermus thermophilus*[J]. Frontiers in Genetics, 2019, 10: 204.

[12] KOGA Y. Thermal adaptation of the archaeal and bacterial lipid membranes[J]. Archaea, 2012, 2012: 789652.

[13] SLOBODKIN A, SLOBODKINA G, ALLIOUX M, ALAIN K, JEBBAR M, SHADRIN V, KUBLANOV I, TOSHCHAKOV S, BONCH-OSMOLOVSKAYA E. Genomic insights into the carbon and energy metabolism of a thermophilic deep-sea bacterium *Deferribacter autotrophicus* revealed new metabolic traits in the phylum *Deferribacteres*[J]. Genes, 2019, 10(11): 849.

[14] TOMITA T. Structure, function, and regulation of enzymes involved in amino acid metabolism of bacteria and archaea[J]. Bioscience, Biotechnology, and Biochemistry, 2017, 81(11): 2050-2061.

[15] TIMR S, MADERN D, STERPONE F. Protein thermal stability[J]. Progress in Molecular Biology and Translational Science, 2020, 170: 239-272.

[16] CHEN Z, WEN B, WANG QH, TONG W, GUO J, BAI X, ZHAO JJ, SUN Y, TANG Q, LIN ZL, LIN L, LIU SQ. Quantitative proteomics reveals the temperature-dependent proteins encoded by a series of cluster genes in *Thermoanaerobacter tengcongensis*[J]. Molecular & Cellular Proteomics: MCP, 2013, 12(8): 2266-2277.

[17] WANG ZW, TONG W, WANG QH, BAI X, CHEN Z, ZHAO JJ, XU NZ, LIU SQ. The temperature dependent proteomic analysis of *Thermotoga maritima*[J]. Public Library of Science ONE, 2012, 7(10): e46463.

[18] XUE Y, XU Y, LIU Y, MA Y, ZHOU P. *Thermoanaerobacter tengcongensis* sp. nov., a novel anaerobic, saccharolytic, thermophilic bacterium isolated from a hot spring in Tengcong, China[J]. International Journal of Systematic and Evolutionary Microbiology, 2001, 51(Pt 4): 1335-1341.

[19] MENG B, QIAN Z, WEI F, WANG WW, ZHOU CQ, WANG ZW, WANG QH, TONG W, WANG Q, MA YH, XU NZ, LIU SQ. Proteomic analysis on the

temperature-dependent complexes in *Thermoanaerobacter tengcongensis*[J]. Proteomics, 2009, 9(11): 3189-3200.

[20] LIU B, WANG C, YANG HH, TAN HR. Establishment of a genetic transformation system and its application in *Thermoanaerobacter tengcongensis*[J]. Journal of Genetics and Genomics, 2012, 39(10): 561-570.

[21] QIAN Z, ZHAO JJ, BAI X, TONG W, CHEN Z, WEI HF, WANG QH, LIU SQ. Thermal stability of glucokinases in *Thermoanaerobacter tengcongensis*[J]. Biomed Research International, 2013, 2013: 646539.

[22] SHI Y, ZHENG DY, XIE JY, ZHANG QJ, ZHANG HJ. Thermal stability of *Thermoanaerobacter tengcongensis* ribosome recycling factor[J]. Protein and Peptide Letters, 2014, 21(3): 285-291.

[23] LIU B, ZHANG YH, ZHANG W. RNA-seq-based analysis of cold shock response in *Thermoanaerobacter tengcongensis*, a bacterium harboring a single cold shock protein encoding gene[J]. Public Library of Science ONE, 2014, 9(3): e93289.

[24] WANG C, JIN CL, ZHANG JH, BAO QY, LIU B, TAN HR. Transcriptomic analysis of *Thermoanaerobacter tengcongensis* grown at different temperatures by RNA sequencing[J]. Journal of Genetics and Genomics, 2015, 42(6): 335-338.

[25] WANG JQ, ZHAO CF, MENG B, XIE JH, ZHOU CQ, CHEN XS, ZHAO K, SHAO JM, XUE YF, XU NZ, MA YH, LIU SQ. The proteomic alterations of *Thermoanaerobacter tengcongensis* cultured at different temperatures[J]. Proteomics, 2007, 7(9): 1409-1419.

[26] NAVDAEVA V, ZURBRIGGEN A, WALTERSPERGER S, SCHNEIDER P, OBERHOLZER AE, BÄHLER P, BÄCHLER C, GRIEDER A, BAUMANN U, ERNI B. Phosphoenolpyruvate: sugar phosphotransferase system from the hyperthermophilic *Thermoanaerobacter tengcongensis*[J]. Biochemistry, 2011, 50(7): 1184-1193.

[27] MIZOTE T, TSUDA M, SMITH DDS, NAKAYAMA H, NAKAZAWA T. Cloning and characterization of the *thiD*/*J* gene of *Escherichia coli* encoding a thiamin-synthesizing bifunctional enzyme, hydroxymethylpyrimidine kinase/phosphomethylpyrimidine kinase[J]. Microbiology, 1999, 145(Pt2): 495-501.

[28] JURGENSON CT, BEGLEY TP, EALICK SE. The structural and biochemical foundations of thiamin biosynthesis[J]. Annual Review of Biochemistry, 2009, 78: 569-603.

[29] NODWELL MB, MENZ H, KIRSCH SF, SIEBER SA. Rugulactone and its analogues exert antibacterial effects through multiple mechanisms including inhibition of thiamine biosynthesis[J]. Chembiochem: a European Journal of Chemical Biology, 2012, 13(10): 1439-1446.

[30] HAAS AL, LAUN NP, BEGLEY TP. Thi20, a remarkable enzyme from *Saccharomyces cerevisiae* with dual thiamin biosynthetic and degradation activities[J]. Bioorganic Chemistry, 2005, 33(4): 338-344.

[31] FRENCH JB, BEGLEY TP, EALICK SE. Structure of trifunctional THI20 from yeast[J]. Acta Crystallographica Section D, Biological Crystallography, 2011, 67(Pt 9): 784-791.

[32] KARUNAKARAN R, EBERT K, HARVEY S, LEONARD ME, RAMACHANDRAN V, POOLE PS. Thiamine is synthesized by a salvage pathway in *Rhizobium leguminosarum* bv. viciae strain 3841[J]. Journal of Bacteriology, 2006, 188(18): 6661-6668.

[33] WANG YG, SUN SC, YU LM, HU S, FAN WG, LENG FF, MA JZ. Optimization and mechanism exploration for *Escherichia coli* transformed with plasmid pUC19 by the combination with ultrasound treatment and chemical method[J]. Ultrasonics Sonochemistry, 2021, 74: 105552.

[34] STEEMERS FJ, GUNDERSON KL. Illumina, Inc.[J]. Pharmacogenomics, 2005, 6(7): 777-782.

[35] LANGMEAD B, TRAPNELL C, POP M, SALZBERG SL. Ultrafast and memory-efficient alignment of short DNA sequences to the human genome[J]. Genome Biology, 2009, 10(3): R25.

[36] PUTRI GH, ANDERS S, PYL PT, PIMANDA JE, ZANINI F. Analysing high-throughput sequencing data in Python with HTSeq 2.0[J]. Bioinformatics, 2022, 38(10): 2943-2945.

[37] ZHAO YD, LI MC, KONATÉ MM, CHEN L, DAS B, KARLOVICH C, WILLIAMS PM, EVRARD YA, DOROSHOW JH, McSHANE LM. TPM, FPKM, or normalized counts? A comparative study of quantification measures for the analysis of RNA-seq data from the NCI patient-derived models repository[J]. Journal of Translational Medicine, 2021, 19(1): 269.

[38] LOVE MI, HUBER W, ANDERS S. Moderated estimation of fold change and dispersion for RNA-seq data with DESeq2[J]. Genome Biology, 2014, 15(12): 550.

[39] GHOSH D. Wavelet-based Benjamini-Hochberg procedures for multiple testing under dependence[J].

Mathematical Biosciences and Engineering: MBE, 2019, 17(1): 56-72.

[40] ANDERS S, HUBER W. Differential expression analysis for sequence count data[J]. Nature Precedings, 2010.

[41] TARAZONA S, GARCÍA-ALCALDE F, DOPAZO J, FERRER A, CONESA A. Differential expression in RNA-seq: a matter of depth[J]. Genome Research, 2011, 21(12): 2213-2223.

[42] KANEHISA M, GOTO S. KEGG: Kyoto encyclopedia of genes and genomes[J]. Nucleic Acids Research, 2000, 28(1): 27-30.

[43] BUCHFINK B, XIE C, HUSON DH. Fast and sensitive protein alignment using DIAMOND[J]. Nature Methods, 2015, 12: 59-60.

[44] JIAO YM, WIDSCHWENDTER M, TESCHENDORFF AE. A systems-level integrative framework for genome-wide DNA methylation and gene expression data identifies differential gene expression modules under epigenetic control[J]. Bioinformatics, 2014, 30(16): 2360-2366.

[45] DEMBSKA A, ŚWITALSKA A, FEDORUK-WYSZOMIRSKA A, JUSKOWIAK B. Development of fluorescence oligonucleotide probes based on cytosine- and guanine-rich sequences[J]. Scientific Reports, 2020, 10: 11006.

[46] DUTTA A, CHAUDHURI K. Analysis of tRNA composition and folding in psychrophilic, mesophilic and thermophilic genomes: indications for thermal adaptation[J]. FEMS Microbiology Letters, 2010, 305(2): 100-108.

[47] BASAK S, MUKHOPADHYAY P, GUPTA SK, GHOSH TC. Genomic adaptation of prokaryotic organisms at high temperature[J]. Bioinformation, 2010, 4(8): 352-356.

[48] MALLIK S, KUNDU S. A comparison of structural and evolutionary attributes of *Escherichia coli* and *Thermus thermophilus* small ribosomal subunits: signatures of thermal adaptation[J]. Public Library of Science ONE, 2013, 8(8): e69898.

[49] LOVERING AL, SAFADI SS, STRYNADKA NCJ. Structural perspective of peptidoglycan biosynthesis and assembly[J]. Annual Review of Biochemistry, 2012, 81: 451-478.

[50] VOLLMER W, BLANOT D, DE PEDRO MA. Peptidoglycan structure and architecture[J]. FEMS Microbiology Reviews, 2008, 32(2): 149-167.

[51] HANSEN T, OEHLMANN M, SCHÖNHEIT P. Novel type of glucose-6-phosphate isomerase in the hyperthermophilic archaeon *Pyrococcus furiosus*[J]. Journal of Bacteriology, 2001, 183(11): 3428-3435.

[52] WYLLIE JA, MCKAY MV, BARROW AS, SOARES DA COSTA TP. Biosynthesis of uridine diphosphate N-acetylglucosamine: an underexploited pathway in the search for novel antibiotics?[J]. IUBMB Life, 2022, 74(12): 1232-1252.

[53] NESTEROV SV, YAGUZHINSKY LS, PODOPRIGORA GI, NARTSISSOV YR. Amino acids as regulators of cell metabolism[J]. Biochemistry, 2020, 85(4): 393-408.

[54] REED CJ, LEWIS H, TREJO E, WINSTON V, EVILIA C. Protein adaptations in archaeal extremophiles[J]. Archaea, 2013, 2013: 373275.

[55] SHIVAJI S, PRAKASH JSS. How do bacteria sense and respond to low temperature?[J]. Archives of Microbiology, 2010, 192(2): 85-95.

[56] FASSLER JS, WEST AH. Histidine phosphotransfer proteins in fungal two-component signal transduction pathways[J]. Eukaryotic Cell, 2013, 12(8): 1052-1060.

[57] RAJPUT A, SEIF Y, CHOUDHARY KS, DALLDORF C, POUDEL S, MONK JM, PALSSON BO. Pangenome analytics reveal two-component systems as conserved targets in ESKAPEE pathogens[J]. mSystems, 2021, 6(1): e00981-20.

[58] BUSCHIAZZO A, TRAJTENBERG F. Two-component sensing and regulation: how do histidine kinases talk with response regulators at the molecular level?[J]. Annual Review of Microbiology, 2019, 73: 507-528.

[59] HOREMANS S, PITOULIAS M, HOLLAND A, PATEAU E, LECHAPLAIS C, EKATERINA D, PERRET A, SOULTANAS P, JANNIERE L. Pyruvate kinase, a metabolic sensor powering glycolysis, drives the metabolic control of DNA replication[J]. BMC Biology, 2022, 20(1): 87.

[60] TANG Q, LIU YP, SHAN HH, TIAN LF, ZHANG JZ, YAN XX. ATP-dependent conformational change in ABC-ATPase RecF serves as a switch in DNA repair[J]. Scientific Reports, 2018, 8: 2127.

[61] MALLIK S, POPODI EM, HANSON AJ, FOSTER PL. Interactions and localization of *Escherichia coli* error-prone DNA polymerase IV after DNA damage[J]. Journal of Bacteriology, 2015, 197(17): 2792-2809.

[62] ZHANG SL, LIU B, YANG HH, TIAN YQ, LIU G, LI L, TAN HR. Characterization of EndoTT, a novel single-stranded DNA-specific endonuclease from *Thermoanaerobacter tengcongensis*[J]. Nucleic Acids

Research, 2010, 38(11): 3709-3720.

[63] WANI AK, AKHTAR N, SHER F, NAVARRETE AA, AMÉRICO-PINHEIRO JHP. Microbial adaptation to different environmental conditions: molecular perspective of evolved genetic and cellular systems[J]. Archives of Microbiology, 2022, 204(2): 144.

[64] KOLIBACHUK D, ROUHBAKHSH D, BAUMANN P. Aromatic amino acid biosynthesis in *Buchnera aphidicola* (endosymbiont of aphids): cloning and sequencing of a DNA fragment containing aroH-thrS-infC-rpmI-rplT[J]. Current Microbiology, 1995, 30(5): 313-316.

[65] ZHAO MN, ZHANG MN, REN ZH, WANG YY, GUAN ZH. Base-mediated formal[3+2]cycloaddition of β, γ-alkenyl esters and p-TsN_3 for the synthesis of pyrazoles[J]. Science Bulletin, 2017, 62(7): 493-496.

[66] ESTEVES AM, GRAÇA G, PEYRIGA L, TORCATO IM, BORGES N, PORTAIS JC, SANTOS H. Combined transcriptomics–metabolomics profiling of the heat shock response in the hyperthermophilic archaeon *Pyrococcus furiosus*[J]. Extremophiles, 2019, 23(1): 101-118.

[67] KOUZMINOVA EA, KADYROV FF, KUZMINOV A. RNase HII saves rnhA mutant *Escherichia coli* from R-loop-associated chromosomal fragmentation[J]. Journal of Molecular Biology, 2017, 429(19): 2873-2894.

[68] LI J, ZHENG W, GU M, HAN L, LUO YM, YU KK, SUN MX, ZONG YL, MA XX, LIU B, LOWDER EP, MENDEZ DL, KRANZ RG, ZHANG K, ZHU JP. Structures of the CcmABCD heme release complex at multiple states[J]. Nature Communications, 2022, 13: 6422.

[69] GONG Z, YANG S, DONG X, YANG QF, ZHU YL, XIAO Y, TANG C. Hierarchical conformational dynamics confers thermal adaptability to $preQ_1$ RNA riboswitches[J]. Journal of Molecular Biology, 2020, 432(16): 4523-4543.